Clinical Radiology 74 (2019) 259–267

Contents lists available at ScienceDirect

Clinical Radiology

journal homepage: www.clinicalradiologyonline.net

MpMRI of the prostate: is there a role for semi-quantitative analysis of DCE-MRI and late gadolinium enhancement in the characterisation of prostate cancer?

G. Cristel [a,*], A. Esposito [a,b], A. Briganti [b,c], A. Damascelli [a,b], G. Brembilla [a,b], M. Freschi [d], A. Ambrosi [b], F. Montorsi [b,c], A. Del Maschio [a,b], F. De Cobelli [a,b]

[a] *Department of Radiology, Experimental Imaging Center, San Raffaele Scientific Institute, via Olgettina 60, 20132 Milan, Italy*
[b] *Vita Salute San Raffaele University, via Olgettina 60, 20132 Milan, Italy*
[c] *Department of Urology, San Raffaele Scientific Institute, via Olgettina 60, 20132 Milan, Italy*
[d] *Department of Pathology, San Raffaele Scientific Institute, via Olgettina 60, 20132 Milan, Italy*

ARTICLE INFORMATION

Article history:
Received 17 January 2018
Accepted 13 August 2018

AIM: To assess whether there is a significant difference in perfusion parameters between benign and malignant prostatic lesions, focusing on semi-quantitative analysis of dynamic contrast-enhanced (DCE) magnetic resonance imaging (MRI) and presence of late gadolinium enhancement (LGE).

MATERIAL AND METHODS: Three hundred and thirteen patients who underwent multiparametric MRI (mpMRI) of the prostate and with available corresponding histology (prostatectomy or biopsy) were selected retrospectively for this study. The MRI protocol consisted of multiplanar T2-and diffusion-weighted imaging, DCE and delayed axial T1 images. Images were reviewed independently by two radiologists for LGE assessment and Prostate Imaging – Reporting and Data System (PI-RADS) scoring. For each lesion, semi-quantitative analysis of DCE-MRI was performed and the following data were evaluated: time to peak, wash-in rate, wash-out rate, brevity of enhancement, and area under the curve. The presence or absence of LGE in delayed axial T1 images was assessed qualitatively. MRI results were compared to histology. The presence of significant prostate cancer was based both on Epstein criteria (SPC) and Gleason score (GS $\geq$7).

RESULTS: SPC and Gleason score $\geq$7 tumours showed significant lower time to peak and brevity of enhancement ($p<0.001$) with higher wash-in rate ($p=0.001$). LGE was observed in 152/313 (49%) cases; among them 103/152 (68%) did not show SPC whereas 49/152 (32%) had SPC ($p<0.001$). The presence of LGE determined a risk reduction of SPC resulting as an independent predictor at multivariate analysis (logOR=-0.78, SE 0.33, $p=0.02$).

* Guarantor and correspondent: G. Cristel, Department of Radiology, San Raffaele Scientific Institute, Vita-Salute San Raffaele University, via Olgettina 60, 20132 Milano, Italy. Tel.: +393483667552.
E-mail address: cristel.giulia@hsr.it (G. Cristel).

https://doi.org/10.1016/j.crad.2018.08.017

CONCLUSION: Semi-quantitative perfusion analysis and LGE may help to predict the presence/absence of a significant prostate tumour and represent a promising tool to improve mpMRI diagnostic performance.

Introduction

Multiparametric magnetic resonance imaging (mpMRI) has emerged in the recent years as a valuable tool for the diagnosis and management of prostate cancer (PCa).[1,2] Similar to other oncological scenarios, mpMRI is characterised by an excellent sensitivity in tumour detection with a high negative predictive value (NPV).[3] On the other hand, its specificity along with its positive predictive value (PPV) are still limited.[4] Indeed, one of the biggest current challenges for mpMRI in PCa is to clearly separate between lesions with different malignancy, which therefore require different therapeutic approaches.[5]

Prostate Imaging – Reporting and Data System (PI-RADS) has been proposed from the American College of Radiology and the European Society of Uroradiology to standardise and diminish variation in the acquisition, interpretation, and reporting of prostate mpMRI. It summarises in a five-point scale the level of suspicion of clinically significant PCa based on mpMRI findings considering T2-weighted (T2W), diffusion-weighted imaging (DWI), and dynamic contrast-enhanced MRI (DCE).[6] In the updated PI-RADS v.2 the role of DCE has been reduced because the kinetics of prostate cancer enhancement are quite variable and heterogeneous, and it has become secondary to DWI and T2W images. DCE is now based on qualitative and subjective assessment of early focal enhancement in a suspicious area in the peripheral zone (PZ)[1,7]; however, DCE is recommended to be included in all prostate mpMRI examinations to avoid missing some significant tumours. Actually, the PI-RADS scoring system tries to classify a spectrum of diseases into standardised categories, which is often a continuum with multiple shades of grey. In this difficult setting, PI-RADS classification (and mpMRI consequently), inevitably denotes remaining limitations, most important being the high number of false positive (FP) results (resulting in sub-optimal specificity and PPV) as well as the inter-reader variability, as previously mentioned.[8]

It is important to remember that the behaviour of DCE reflects the histology of the tissue under examination. In the case of PCa, there is an increase in both density and permeability of blood vessels.[9,10] These microvascular alterations result in different enhancement patterns of PCa compared with benign prostate tissue, when performing DCE-MRI. These differences include[1] earlier and more intense enhancement and[2] more rapid washout of contrast medium within the tumour.[11] On the other hand, many patients undergoing mpMRI for PCa investigation present with benign post-inflammatory chronic prostate remodelling (e.g., due to previous prostatitis) which, different to PCa, are characterised by increased extracellular space volume with tissue fibrosis due to myofibroblast accumulation, collagen deposition, extracellular matrix (ECM) remodelling, and increased tissue stiffness.[12] These alterations represent the typical challenging FP results of prostate mpMRI.

Over the years, subsequent refinements have been added to mpMRI to improve its performance. For instance, semi-quantitative and quantitative DCE parameters have been proven to be useful for the characterisation and grading of PCa,[13,14] although they still do not allow to address borderline and benign lesions precisely.

Looking for tools to better characterise fibrotic lesions, the present authors turned to another MRI field in which scars have been studied extensively: cardiac MRI. In cardiac MRI, myocardial fibrosis can be recognised accurately and quantified by probing the retention of gadolinium-contrast agent in myocardial tissue (late-gadolinium enhancement, LGE).[15] Deriving this concept from cardiac MRI, the present study was undertaken to evaluate if LGE could increase the ability of mpMRI to differentiate benign fibrotic lesions from PCa. The aim of the study was to assess whether there is a significant difference in perfusion parameters and contrast medium retention between benign and malignant prostatic lesions, particularly focusing on semi-quantitative analysis of DCE-MRI and LGE presence.

Materials and methods

Patient population

The Institutional Review Board approved this retrospective study. Archived patient data from the institutional database were used. All men undergoing mpMRI of the prostate at San Raffaele Scientific Institute (and consequently enrolled in this analysis) provided written informed consent for having their data collected for research purposes before the examination. Among a total of 796 men who underwent prostate mpMRI at San Raffaele Scientific Institute between January 2012 and May 2016, all patients with an available corresponding histological specimen, obtained through radical prostatectomy (n=92; 29%), post-MRI targeted 18-core biopsies (n=77; 25%), or pre-MRI (n=144; 46%) transrectal ultrasound (TRUS) 12 core (n=44) or 16-core (n=100) needle biopsies were selected. Those men (n=470) without histological validation (not performed or discordant in location) were deliberately excluded from the analysis. From the resulting 326 patients, those treated with anti-androgen therapy (n=7) and those with poor quality imaging (n=6) were also excluded. The final population consisted of 313 patients. In cases of

multifocal disease, only the index lesion was considered for analysis. Prostate specimens were processed according to the Stanford protocol[16] and analysed by a dedicated uropathologist with 20 years of experience.

MRI protocol

All patients underwent a 1.5 T mpMRI study (Achieva and Achieva dStream, Philips Medical Systems, Best, The Netherlands) with a ballon-covered expandable endorectal coil (BPX-15, Bayer Medical Care, Indianola, PA, USA). Gastrointestinal peristalsis was suppressed by intramuscular administration of 20 mg scopolamine-butylbromide (Buscopan, Boehringer Ingelheim, Ingelheim, Germany) in all men. Since September 2015, a phased-array 32-channel surface coil was added (n=91). According to the European Society of Urogenital Radiology guidelines,[6] the imaging protocol included multiplanar turbo spin-echo T2-weighted images, echo-planar DWI (with different b-values: 0/50-800-1400/1600 s/mm^2 and the ADC map automatically created on a pixel-by-pixel basis using both two and three b-values), three-dimensional (3D) fast field-echo DCE MRI (temporal resolution 4.1 seconds) and delayed axial turbo spin echo T1-weighted images with fat suppression. For DCE-MRI, an intravenous bolus of 0.1 mmol/kg gadobutrol (Gadovist, Bayer Schering Pharma, Germany) at 2 ml/s was administered with an automatic injector (Spectris MRI Injector System, Medrad, Indianola, PA, USA), followed by 20 ml saline at the same injection rate. The details of the imaging protocol are listed in Table 1. All mpMRI examinations were performed after at least 4 weeks from prostate biopsy, in order to minimise post-biopsy haemorrhagic artefacts.

MRI image analysis

Images were reviewed independently for the LGE assessment and PI-RADS scoring by two radiologists with 10 and 2 years of experience on prostate mpMRI interpretation, respectively, who knew the location of the index lesion, but were blinded to clinical (PSA, clinical stage, previous biopsies) and histopathological information (number of positive specimens, percentage of tumoural tissue per specimen, and location of the lesion). All images were reported according to PI-RADS v. 2 guidelines.[1] Of note, histopathological data were available for all the target areas included in the present study. A third experienced radiologist (20 years of experience) had previously selected the index lesions (i.e., lesion with greater PI-RADS score) and matched them with the corresponding histopathology. The same radiologist was in consulted to provide a decision in cases of disagreement between the two readers.

ROIs (region of interest) were drawn manually by the reader with 10 years of experience on the subtracted image sets from the DCE-MRI using T2-weighted images or ADC map for the morphologic reference, in order to identify the lesions. ADC analysis and perfusion measurements were assessed for each resulting ROI using commercial image-viewing software (IntelliSpace Portal v.7, Philips Healthcare). The graphical results showed a time–Intensity diagram. For the semi-quantitative analysis, the following parameters were calculated: maximum contrast enhancement (Max Enh), time to maximum contrast enhancement (time to peak [TTP]), speed of contrast uptake (wash-in rate), clearance rate of contrast agent (wash-out rate), time between point of maximum wash-in rate and maximum wash-out rate (brevity of enhancement), and the sum of all intensities under the curve (area under the curve [AUC]). A graphic overview of these parameters is presented in Fig 1. LGE was assessed visually for each lesion using delayed axial T1-weighted images and defined as the presence of focal hyperintensity of the target area compared to the surrounding tissue.

MRI results were compared to histology. Significant PCa was defined according to Epstein criteria (SPC; definition of insignificant prostate carcinoma: PSA density $<$0.15 ng/ml, Gleason score $\leq$6, fewer than three cores containing PCa and $\leq$50% involvement of any core with prostate carcinoma)[17] and Gleason score (GS $\geq$7 or International Society of Urological Pathology (ISUP) grade group $\geq$ 2,[18]).

Statistical analysis

The observed clinical and demographic continuous data were reported by means of mean values $\pm$ the standard deviation or as median (interquartile range), categorical data as frequencies and percentages. Interobserver agreement for PI-RADS scoring and LGE evaluation was assessed

Table 1
Imaging protocol details.

Parameters	TSE T2-W axial	TSE T2-W sagittal	TSE T2-W coronal	DWI (b: 0/50, 800, 1400/1600)	DCE	TSE T1-W axial
TR (ms)	4,824	4,370	2,991	4,376	3.7	4.4
TE (ms)	120	120	120	80	1.83	2.2
FOV (mm)	180×180	180×180	180×180	180×180	180×180	295×357
Matrix	512×512	512×512	512×512	144×144	288×288	560×560
Thickness (mm)	3	3	3	3	3	1.5
Gap (mm)	0.3	0.3	0.3	0.3	0	0
Flip angle (°)	90	90	90	90	8/5,8,12,15	10
Acquisition time	4 min 6 s	3 min 25 s	2 min 8 s	5 min 19 s	3 min 20 s	1 min 26 s
No. of dynamic scans	—	—	—	—	48	—
Dynamic scan time (s)	—	—	—	—	4	—

Dash indicates data not available.
TSE, turbo spin-echo; DWI, diffusion-weighted imaging; DCE, dynamic contrast enhanced.

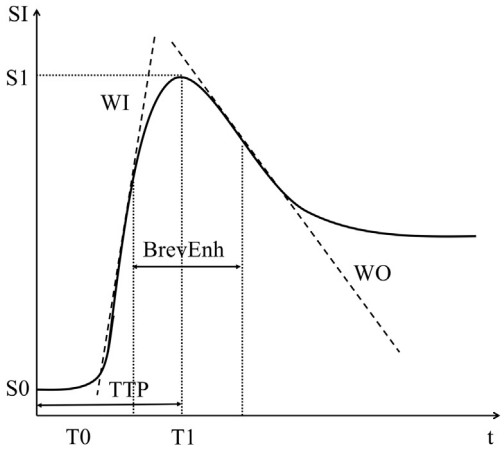

Figure 1 Graphic overview of semi-quantitative DCE-MRI parameters. TTP, time to peak; WI, wash-in rate; WO, wash-out rate; BrevEnh, brevity of enhancement; SI, signal intensity; t, time.

using Cohen's Kappa. Differences in the analysed parameters between benign and malignant groups were calculated using the Mann–Whitney *U*-test or Kruskal–Wallis *H*-test when appropriate. Categorical variables were analysed using χ^2 test. Sensitivity, specificity, NPV, PPV, and accuracy of PI-RADS classification for tumour detection relative to the histopathology reference standard were calculated. To assess the independent contribution of each variable to malignancy at histopathology, a multivariate logistic model was selected by a backward-forward stepwise procedure. Statistical significance was set at $p<0.05$. *p*-Values were computed by permutation procedures, to avoid any distributional assumption. All statistical analyses were performed using SPSS software package version 20.0 (IBM, Armonk, NY, USA) and R (R Foundation for Statistical Computing, Wien, Austria).

Results

Table 2 shows clinical characteristics and GS distribution of the population enrolled in the study ($n=313$). Interobserver agreement was K=0.794 ($p<0.001$) for PI-RADS scoring and K=0.682 ($p<0.001$) for LGE evaluation. Lesion location, PI-RADS classification, and LGE evaluation are summarised in Table 3. Sensitivity, specificity, NPV, PPV, and accuracy of PI-RADS classification are reported in Table 4.

DWI analysis revealed that ADC was significantly lower in patients with Gleason ≥7 compared to Gleason <7 (median ADC=0.74±0.21 versus $0.93\pm0.24\times10^{-3}$ mm^2/s, respectively; $p<0.001$) as well as in case of SPC compared to insignificant tumour (median ADC=0.74±0.21 versus $0.98\pm0.22\times10^{-3}$ mm^2/s, respectively; $p<0.001$). The ADC values were significantly lower in TP cases of PI-RADS classification for Gleason ≥7 compared with FP ones ($p=0.001$).

Semi-quantitative perfusion analysis

In the semi-quantitative analysis, malignant lesions (Gleason ≥7 and SPC) showed earlier TTP ($p<0.001$) and reduced brevity of enhancement ($p=0.001$), with higher wash-in rate ($p<0.001$) compared to the benign or less aggressive lesions (Table 5). Dividing patients according to GS groups (<6, 6, and >6), TTP and brevity of enhancement were significantly lower in more aggressive tumours ($p<0.001$ and $p=0.015$, respectively), with a wash-in rate significantly higher ($p<0.001$). Similar results were observed when classifying patients according to histopathology (negative, insignificant PCa and SPC): TTP $p<0.001$, brevity of enhancement $p=0.010$, wash-in rate $p<0.001$ (Fig 2).

Considering FP and TP of PI-RADS classification for Gleason ≥7, FP showed higher TTP and brevity of enhancement ($p=0.009$ and $p=0.005$ respectively) and lower wash-in rate ($p=0.01$), compared to TP cases.

Table 2
Patient clinical characteristics and histopathological data.

Characteristic	Value
Age (years)	
Mean±SD	64.3±7.5
Range	42–81
PSA (ng/ml)	
Mean±SD	9.5±8.9
Range	0.7–83.8
Prostate volume (cm^3)	
Mean	51.7±26.6
Range	11.9–177.9
Histological result	
Negative	84 (26.8)
ASAP/HG-PIN	28 (8.9)
GS 6	66 (21.1)
GS 7	94 (30)
3+4	38 (12)
4+3	56 (18)
GS 8	18 (5.8)
GS 9	23 (7.3)
GS ≥7	135 (43.1)
SPC	157 (50.2)

PSA, prostate specific antigen; SPC, significant prostate cancer; ASAP/HG-PIN, ASAP, Atypical small acinar proliferation; HG-PIN, High grade prostatic intraepithelial neoplasia; GS, Gleason score.

Table 3
Lesion characteristics at mpMRI.

Characteristic	No. (%) of patients
Location	
PZ	244 (78%)
TZ	69 (22%)
PI-RADS	
2	101 (32.3)
3	54 (17.3)
4	103 (32.9)
5	55 (17.6)
PI-RADS 2 versus 3-4-5	
2	101 (32.3)
3-4-5	212 (67.7)
GS prevalence stratified by PI-RADS	
2	98 GS <7; 3 GS ≥ 7
3	41 GS <7; 13 GS ≥ 7
4	34 GS <7; 69 GS ≥ 7
5	5 GS <7; 50 GS ≥ 7
Late enhancement	
Absent	161 (51.4)
Present	152 (48.6)

GS, Gleason score; PZ, peripheral zone; TZ, transition zone. Data are shown as n (%).

Table 4
Diagnostic accuracy of PI-RADS classification.

	n	TP	FP	TN	FN	Sensitivity	Specificity	PPV	NPV	Accuracy
Gleason score ≥7	313	132	80	98	3	0.98	0.55	0.62	0.97	0.73
Significant prostate cancer	313	153	59	97	4	0.97	0.62	0.72	0.96	0.80

Data assume PI-RADS ≥3 as pathological.
TP, true positive; TN, true negative, FP, false positive; FN, false negative; NPV, negative predictive value; PPV, positive predictive value.

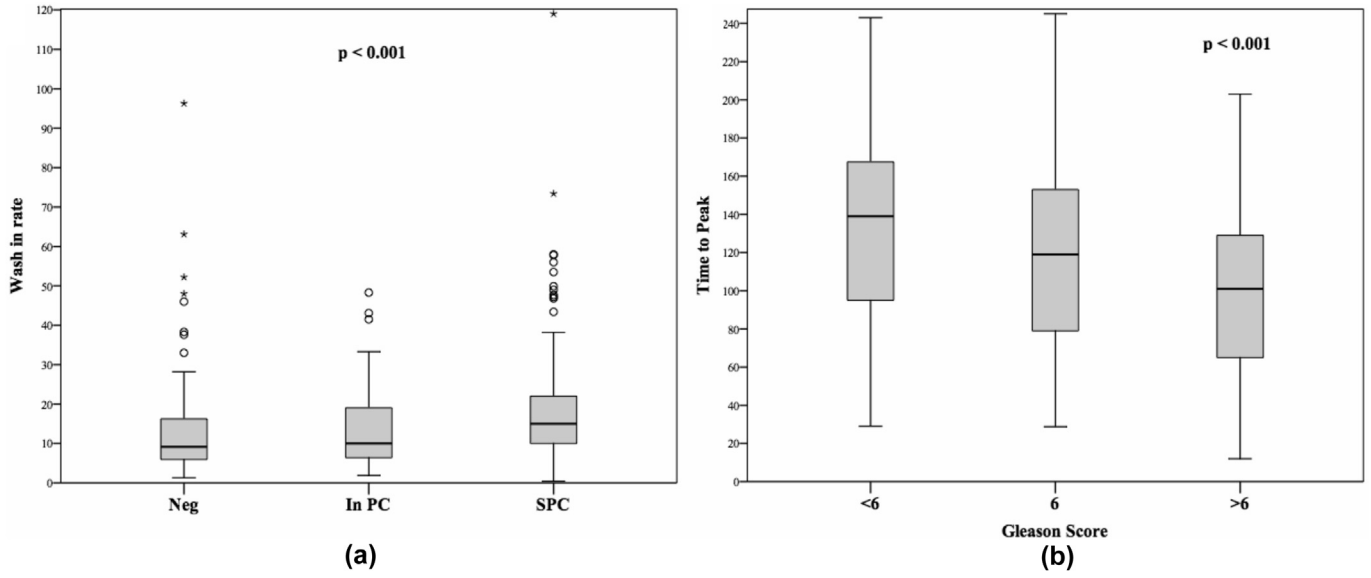

Figure 2 (a) Boxplots showing distribution of wash-in rate according to negative histopathological result (Neg), insignificant prostate cancer (In PC) and significant prostate cancer (SPC). (b) Boxplots showing distribution of TTP according to Gleason score.

LGE evaluation

LGE was observed in 152/313 (49%) cases overall. Among patients with LGE, 44/152 (29%) had Gleason score ≥7 tumour, whereas the remaining 108/152 (71%) had no tumour (84/108) or a tumour with a Gleason score <7 (24/108; $p<0.001$; Fig 3a); histological specimens of the 84 benign alterations revealed areas of atrophy, fibrosis, and chronic inflammation (Figs 4 and 5).

Similarly, 103/152 (68%) patients with LGE did not show SPC whereas only 49/152 (32%) had SPC ($p<0.001$). In the present population, there was no significant difference in LGE presence between FP and TP cases considering Gleason ≥7 ($p=0.078$) even considering only the lesions in PZ ($p=0.078$), but the absence of LGE predicted increased chance of having a FN result (logOR= 1.34, SE 0.36, $p<0.001$).

Considering the group of intermediate risk lesions classified as PI-RADS 3 ($n=54$), LGE was observed in 27 (50%) cases. Among them 23/27 (85%) showed no tumour or a tumour with a Gleason score <7 at histology, (Fig 3b).

Table 6 shows the results from the univariate and multivariate analysis. At multivariate analysis, LGE was confirmed to be an independent predictor of absence of SPC (logOR=−0.78, SE 0.33, $p=0.021$), along with high ADC values ($p<0.001$), low wash-in rate ($p=0.028$), high brevity of enhancement ($p<0.001$), and PI-RADS <3 ($p<0.001$).

Discussion

The main finding of the present study was that the presence of LGE in prostate mpMRI was an independent predictor of the absence of SPC. As previously reported, ADC

Table 5
Values of semi-quantitative analysis parameters in each subgroup.

	GS <7	GS ≥7	*p*-Value	In PC	SPC	*p*-Value
Max Enh	63 (38, 231)	79 (48, 301)	0.08	63 (38, 231)	78 (46, 283)	0.06
Time to peak (s)	130 (86, 165)	101 (65, 129)	<0.001	136 (93, 167)	102 (66, 129)	<0.001
Wash-in rate (l/s)	9 (6, 16)	15 (10, 22)	<0.001	9 (6, 16)	15 (10, 22)	<0.001
Wash-out rate (l/s)	1 (0, 2)	1 (0, 2)	0.72	1 (0, 2)	1 (0, 2)	0.16
Brevity of Enh (s)	108 (52, 145)	78 (30, 117)	0.001	109 (50, 149)	79 (35, 122)	0.003
AUC	2,992 (1,493, 31,810)	3,021 (1,726, 41,516)	0.38	2,788 (1,440, 31,661)	3,344 (1,739, 41,466)	0.12

Data are shown as median (interquartile range).
SPC, significant prostate cancer; In PC, insignificant prostate cancer; GS, Gleason score, Enh, enhancement; AUC, area under the curve.

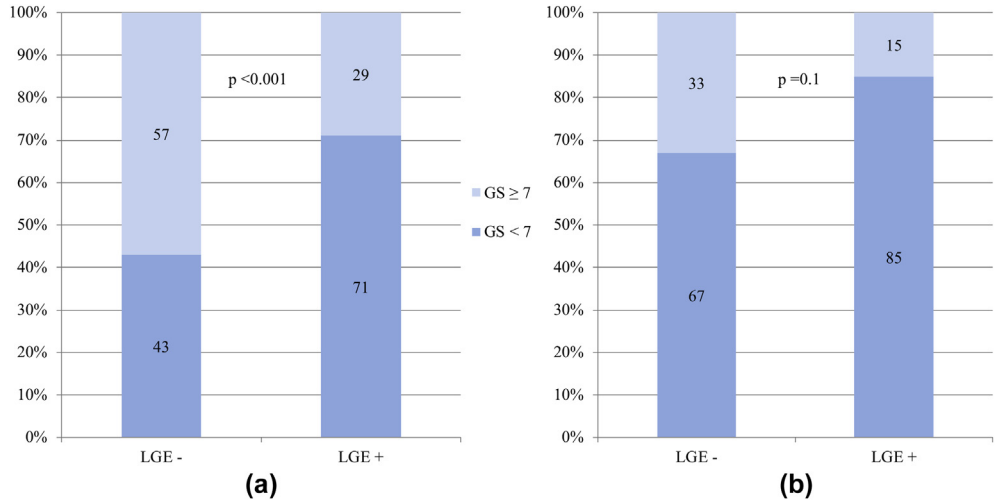

Figure 3 Association between LGE and histopathological result in the overall study population (a) and in the sub-group of PI-RADS 3 (b). (a) In the LGE+ group (n=152), 44/152 (29%) lesions had Gleason score ≥7 and the remaining 108/152 (71%) had Gleason score <7. In the LGE− group (n=161), 91/161 (57%) lesions had Gleason score ≥7 and 70/161 (43%) had Gleason score <7. (b) LGE was observed in 27 (50%) cases in the group of PI-RADS 3 (n=54). Among them 23/27 (85%) showed no tumour or a tumour with a Gleason score <7 at histology.

was confirmed to be one of the strongest predictors of SPC.[5,19,20] Semi-quantitative parameters such as wash-in rate, TTP, and brevity of enhancement have also been already associated with PCa.[13,21–24] These parameters reflect the increased blood supply in the cancerous area due to neoangiogenesis, which determines an increase in both density and permeability of blood vessels within the tissue.[10] The present study confirmed the association between semi-quantitative parameters and SPC. Although they emerged as independent predictors of SPC at multivariate

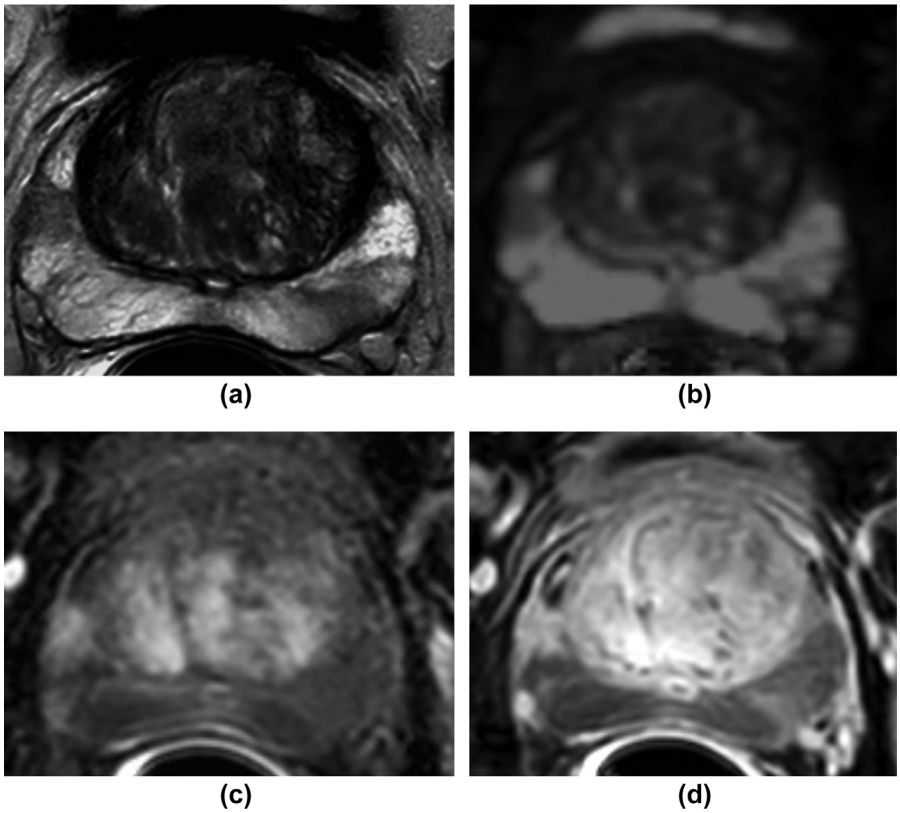

Figure 4 FP case of PI-RADS classification with LGE. Images of a 60-year-old patient with rising PSA (7 ng/ml) and previously negative biopsies. (a) Axial T2-weighted image shows a small ill-defined hypointensity of right PZ with diffusion restriction (b) and focal enhancement at DCE-MRI (c) classified as PI-RADS 4 lesion. (d) In the delayed T1-weighted image, the lesion presented LGE compared to the surrounding PZ. Targeted biopsy was performed showing absence of pathological tissue with atrophy and fibrosis.

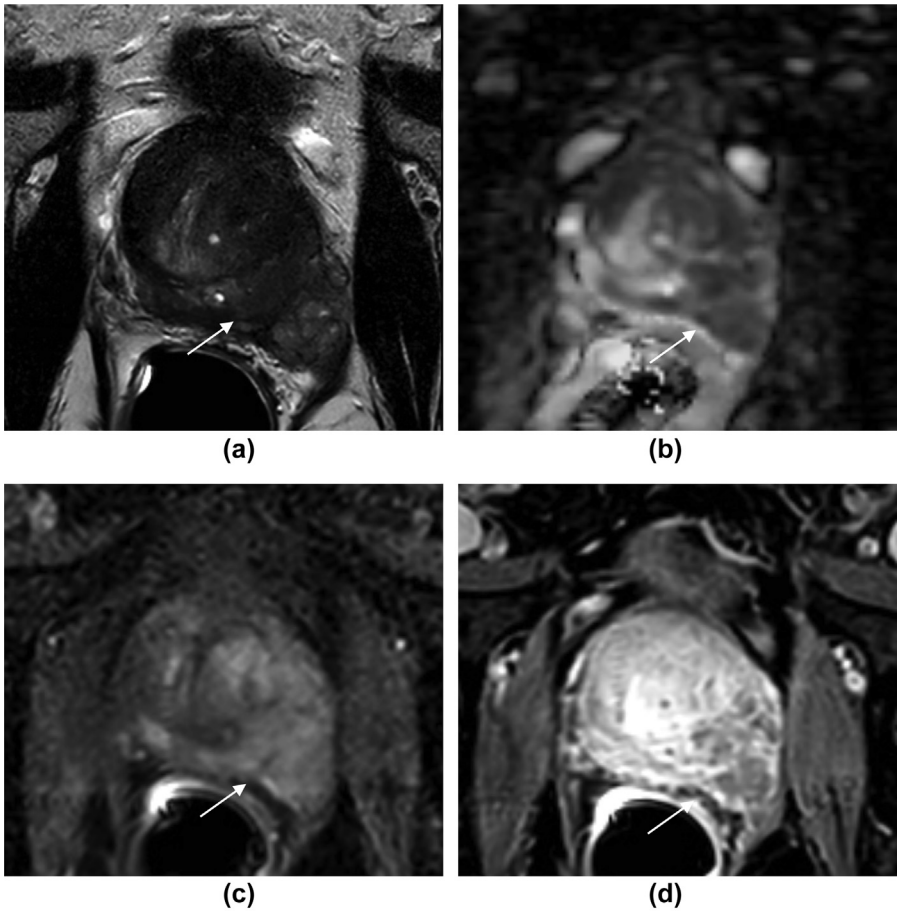

Figure 5 TP case of PI-RADS classification without LGE. Images of a 70-year-old patient with elevated PSA values (27 ng/ml). The arrows show a large lesion in the left PZ with extracapsular extension on T2-weighted imaging (a), restricted diffusion (b), and focal enhancement on DCE-MRI (c) scored as PI-RADS 5. In the delayed T1-weighted image (d) the lesion did not present LGE. A subsequent targeted biopsy confirmed the presence of Gleason 4+5 adenocarcinoma.

analysis, considerable overlap between tumour and benign tissue exists. Brevity of enhancement includes by definition the concepts of "wash-in" and "wash-out" rate, but the "wash-out" parameter alone was not significantly associated with malignancy in the present study. To the authors' knowledge, there are no data on the role of semi-quantitative parameters in the subgroup of FP and TP cases of the PI-RADS classification.

Table 6
Univariate and multivariate analysis in predicting significant prostate cancer.

	Univariate analysis			Multivariate analysis		
	logOR	SE	*p*-Value	logOR	SE	*p*-Value
ADC ($\times 10^{-3}$ mm^2/s)	−4.220	0.650	<0.001	−3.632	0.834	<0.001
PSA (ng/ml)	0.030	0.016	0.065	-	-	-
Late Enh	−1.450	0.240	<0.001	−0.781	0.339	0.021
Max Enh	0.001	0.001	0.360	-	-	-
Time to peak (l/s)	− 0.013	0.003	<0.001	-	-	-
Wash-in rate (l/s)	0.020	0.010	0.006	0.026	0.012	0.028
Wash-out rate (l/s)	− 0.015	0.023	0.500	-	-	-
Brevity of Enh (l/s)	− 0.005	0.002	0.008	−0.011	0.003	<0.001
PI-RADS ≥3	4.140	0.530	<0.001	3.308	0.574	<0.001

ADC, apparent diffusion coefficient; PSA, prostate specific antigen; Enh, enhancement; PI-RADS, Prostate Imaging – Reporting and Data System.

In the setting of prostate mpMRI, the number of cases that remain uncertain and especially of those that end up to be FPs, is still remarkably high: as a matter of fact, MRI specificity ranges approximately from 95% down to 11% across the literature.[25,26] In this scenario of shades of grey and overlapping data, the addition of LGE could improve the identification of TN lesions. The application of LGE in the setting of prostate MRI has yet to be reported. As mentioned above, it is known from cardiac MRI studies that whereas gadolinium-contrast uptake within the first few seconds of administration depends on the tissue perfusion properties, contrast medium retention depends on the amount of extracellular space. Increased interstitial fibrosis and the consequent expansion of extracellular space, result in greater contrast retention that translates into brighter spots in delayed T1-weighted image compared to the surrounding non-scarred tissue.[27] Similarly to the heart, prostatic fibrosis is characterised by ECM remodelling.[12]

Borrowing the LGE concept from cardiac MRI and considering that PCa is known to show significantly higher signal intensity decrease compared to normal prostatic tissue, LGE was analysed in delayed T1-weighted images in order to differentiate benign post-inflammatory findings,

such as fibrosis and chronic prostatitis, from cancer. Histological specimens of alterations positive for LGE showed the presence of areas of atrophy, fibrosis, and chronic inflammation in most of cases. Indeed, the presence of LGE reduced the risk of having SPC and Gleason score ≥7.

In cancer there is sometimes a component of interstitial stromal reaction that is similar to a generic wound repair response with elevated production of extracellular components and ECM remodelling enzymes.[28,29] This interstitial reaction causes contrast medium retention and could be a possible explanation for the presence of clinically significant PCa in 30% of patients with positive LGE.

The application of LGE would be particularly interesting in intermediate and indeterminate lesions, in which conventional PI-RADS often struggles. In the present series, the ability of LGE to predict the absence of disease was especially apparent in the PI-RADS 3 subset: out of 27 lesions LGE+, 23 (85%) were indeed free from disease. The so-called PI-RADS 3+1 of the PZ may represent another setting in which LGE may be especially useful. Typically, in these cases PI-RADS 3 is taken up one grade by the presence of DCE, and they are problematic for conventional PI-RADS system as they are frequently inflammatory related. The addition of LGE may help to downgrade or confirm such uncertain lesions. Although the present preliminary results are promising, the small patient cohort did not permit any reliable statistical analysis and no definitive conclusions can be drawn regarding the potential benefit of LGE in uncertain (PI-RADS 3 and 3+1) lesions. Future studies focused on this particular setting will be required to elucidate this. Although it is clear that LGE cannot be used as a sole parameter, it could be a helpful tool to increase the probability of benign findings in a multiparametric probability model, without causing excessive extension to the length of the examination. This would in turn lead to a subsequent reduction of redundant biopsies and repeated examinations.

Some limitations of the present study must be acknowledged. First, its retrospective nature may have introduced some biases, particularly in patient selection. In particular, no healthy prostate tissue (PI-RADS 1) was included as a control in the analysis. Second, given the relatively small numbers in the present series, the findings need to be validated using a larger dataset. Additionally, histopathological data (reference standard) was carried out through different procedures (radical prostatectomy in a third of the patients and TRUS-guided or targeted biopsies in the remaining). Moreover, as the examinations have been acquired over a period of 4 years (2012–2016), some variability in the imaging acquisition protocols has been introduced. The evaluation of LGE was qualitative and by definition exposed to inter-reader variability. It would be interesting to apply a quantitative approach with dedicated sequences evaluating the extracellular extravascular volume fraction (Ve) or using the standard deviation of signal intensity to automatically detect the presence of LGE.[30]

In conclusion, semi-quantitative parameters derived from DCE-MRI were confirmed to strengthen PI-RADS classification. The presence of LGE predicted the absence of SPC and could represent a new promising tool to enhance the diagnostic accuracy of mpMRI in the setting of PCa.

Declarations of interest

None.

Funding

This research did not receive any specific grant from funding agencies in the public, commercial, or not-for-profit sectors.

References

1. Weinreb JC, Barentsz JO, Choyke PL, *et al*. PI-RADS prostate imaging – reporting and data system: 2015, version 2. *Eur Urol* 2016;**69**(1):16–40.
2. Johnson LM, Turkbey B, Figg WD, *et al*. Multiparametric MRI in prostate cancer management. *Nat Rev Clin Oncol* 2014;**11**(6):346–53.
3. Abd-Alazeez M, Ahmed HU, Arya M, *et al*. The accuracy of multiparametric MRI in men with negative biopsy and elevated PSA level—can it rule out clinically significant prostate cancer? *Urol Oncol* 2014;**32**(1):45. e17-22.
4. Ahmed HU, El-Shater Bosaily A, Brown LC, *et al*. Diagnostic accuracy of multi-parametric MRI and TRUS biopsy in prostate cancer (PROMIS): a paired validating confirmatory study. *Lancet* 2017;**389**(10071):815–22.
5. Oto A, Yang C, Kayhan A, *et al*. Diffusion-weighted and dynamic contrast-enhanced MRI of prostate cancer: correlation of quantitative MRI parameters with Gleason score and tumour angiogenesis. *AJR Am J Roentgenol* 2011;**197**(6):1382–90.
6. Barentsz JO, Richenberg J, Clements R, *et al*. ESUR prostate MRI guidelines 2012. *Eur Radiol* 2012;**22**(4):746–57.
7. Barrett T, Turkbey B, Choyke PL. PI-RADS version 2: what you need to know. *Clin Radiol* 2015;**70**(11):1165–76.
8. Rosenkrantz AB, Ginocchio LA, Cornfeld D, *et al*. Interobserver reproducibility of the PI-RADS Version 2 lexicon: a multicenter study of six experienced prostate radiologists. *Radiology* 2016;**280**(3):793–804.
9. Hoeks CM, Barentsz JO, Hambrock T, *et al*. Prostate cancer: multiparametric MRI for detection, localization, and staging. *Radiology* 2011;**261**(1):46–66.
10. Dewhirst MW, Tso CY, Oliver R, *et al*. Morphologic and hemodynamic comparison of tumour and healing normal tissue microvasculature. *Int J Radiat Oncol Biol Phys* 1989;**17**(1):91–9.
11. Engelbrecht MR, Huisman HJ, Laheij RJ, *et al*. Discrimination of prostate cancer from normal peripheral zone and central gland tissue by using dynamic contrast-enhanced MRI. *Radiology* 2003;**229**(1):248–54.
12. Rodriguez-Nieves JA, Macoska JA. Prostatic fibrosis, lower urinary tract symptoms, and BPH. *Nat Rev Urol* 2013;**10**(9):546–50.
13. Kim SH, Choi MS, Kim MJ, *et al*. Role of semi-quantitative dynamic contrast-enhanced MRI in characterization and grading of prostate cancer. *Eur J Radiol* 2017;**94**:154–9.
14. Hauth E, Halbritter D, Jaeger H, *et al*. Diagnostic value of semi-quantitative and quantitative analysis of functional parameters in multiparametric MRI of the prostate. *Br J Radiol* 2017;**90**(1078):20170067.
15. Kim RJ, Fieno DS, Parrish TB, *et al*. Relationship of MRI delayed contrast enhancement to irreversible injury, infarct age, and contractile function. *Circulation* 1999;**100**(19):1992–2002.
16. Srigley JR, Humphrey PA, Amin MB, *et al*. Protocol for the examination of specimens from patients with carcinoma of the prostate gland. *Arch Pathol Lab Med* 2009;**133**(10):1568–76.
17. Epstein JI, Walsh PC, Carmichael M, *et al*. Pathologic and clinical findings to predict tumour extent of nonpalpable (stage T1c) prostate cancer. *JAMA* 1994;**271**(5):368–74.
18. Epstein JI, Egevad L, Amin MB, *et al*. The 2014 International society of urological pathology (ISUP) consensus conference on gleason grading of prostatic carcinoma: definition of grading patterns and proposal for a new grading system. *Am J Surg Pathol* 2016;**40**(2):244–52.

19. Langer DL, van der Kwast TH, Evans AJ, *et al*. Prostate cancer detection with multi-parametric MRI: logistic regression analysis of quantitative T2, diffusion-weighted imaging, and dynamic contrast-enhanced MRI. *J Magn Reson Imag* 2009;**30**(2):327–34.
20. De Cobelli F, Ravelli S, Esposito A, *et al*. Apparent diffusion coefficient value and ratio as noninvasive potential biomarkers to predict prostate cancer grading: comparison with prostate biopsy and radical prostatectomy specimen. *AJR Am J Roentgenol* 2015;**204**(3):550–7.
21. Vos EK, Litjens GJ, Kobus T, *et al*. Assessment of prostate cancer aggressiveness using dynamic contrast-enhanced magnetic resonance imaging at 3 T. *Eur Urol* 2013;**64**(3):448–55.
22. Isebaert S, De Keyzer F, Haustermans K, *et al*. Evaluation of semi-quantitative dynamic contrast-enhanced MRI parameters for prostate cancer in correlation to whole-mount histopathology. *Eur J Radiol* 2012;**81**(3):e217–22.
23. Hoang Dinh A, Melodelima C, Souchon R, *et al*. Quantitative analysis of prostate multiparametric MRI images for detection of aggressive prostate cancer in the peripheral zone: a multiple imager study. *Radiology* 2016;**280**(1):117–27.
24. Chen YJ, Chu WC, Pu YS, *et al*. Washout gradient in dynamic contrast-enhanced MRI is associated with tumour aggressiveness of prostate cancer. *J Magn Reson Imag* 2012;**36**(4):912–9.
25. de Rooij M, Hamoen EH, Futterer JJ, *et al*. Accuracy of multiparametric MRI for prostate cancer detection: a meta-analysis. *AJR Am J Roentgenol* 2014;**202**(2):343–51.
26. Moldovan PC, Van den Broeck T, Sylvester R, *et al*. What is the negative predictive value of multiparametric magnetic resonance imaging in excluding prostate cancer at biopsy? A systematic review and meta-analysis from the European association of urology prostate cancer guidelines panel. *Eur Urol* 2017;**72**(2):250–66.
27. Ambale-Venkatesh B, Lima JA. Cardiac MRI: a central prognostic tool in myocardial fibrosis. *Nat Rev Cardiol* 2015;**12**(1):18–29.
28. Tuxhorn JA, Ayala GE, Smith MJ, *et al*. Reactive stroma in human prostate cancer: induction of myofibroblast phenotype and extracellular matrix remodeling. *Clin Cancer Res* 2002;**8**(9):2912–23.
29. Kruslin B, Ulamec M, Tomas D. Prostate cancer stroma: an important factor in cancer growth and progression. *Bosn J Basic Med Sci* 2015; **15**(2):1–8.
30. Amado LC, Gerber BL, Gupta SN, *et al*. Accurate and objective infarct sizing by contrast-enhanced magnetic resonance imaging in a canine myocardial infarction model. *J Am Coll Cardiol* 2004;**44**(12):2383–9.